

8. UV response of PVDF/ZnO composite

8.1. Optical transmission of PVDF and PVDF/ZnO composite

Optical transmissions of PVDF and PVDF/ZnO composite are measured by UV-Vis spectrometer in the wavelength region of 200 – 800 nm and are shown in fig. 8.1. For both PVDF and PVDF/ZnO, a broad absorption is observed with maximum absorption at 320 nm which lies in the UV region. There is a sharp absorption edge at ~ 310 nm is observed for both PVDF and PVDF/ZnO composite. On the other side of the spectra, gradual and slow fall in absorption up to 850 nm is observed. This absorption of UV light is due to electronic transition of electrons.

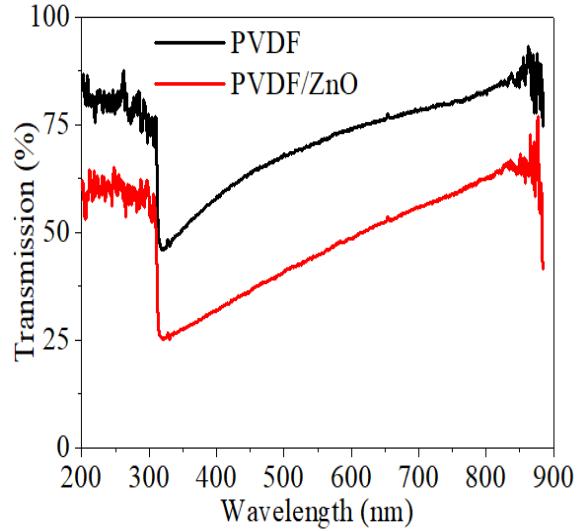


Fig. 8.1 Optical transmission of PVDF and PVDF/ZnO composite films

8.2. UV response of PVDF and PVDF/ZnO composite

Time dependent rise and fall curves of UV response of PVDF and PVDF/ZnO composite were measured when placed under UV light source of power density $\sim 8.3 \mu\text{W}/\text{cm}^2$. Useful parameters obtained from these measurements are presented in Table – 8.1.

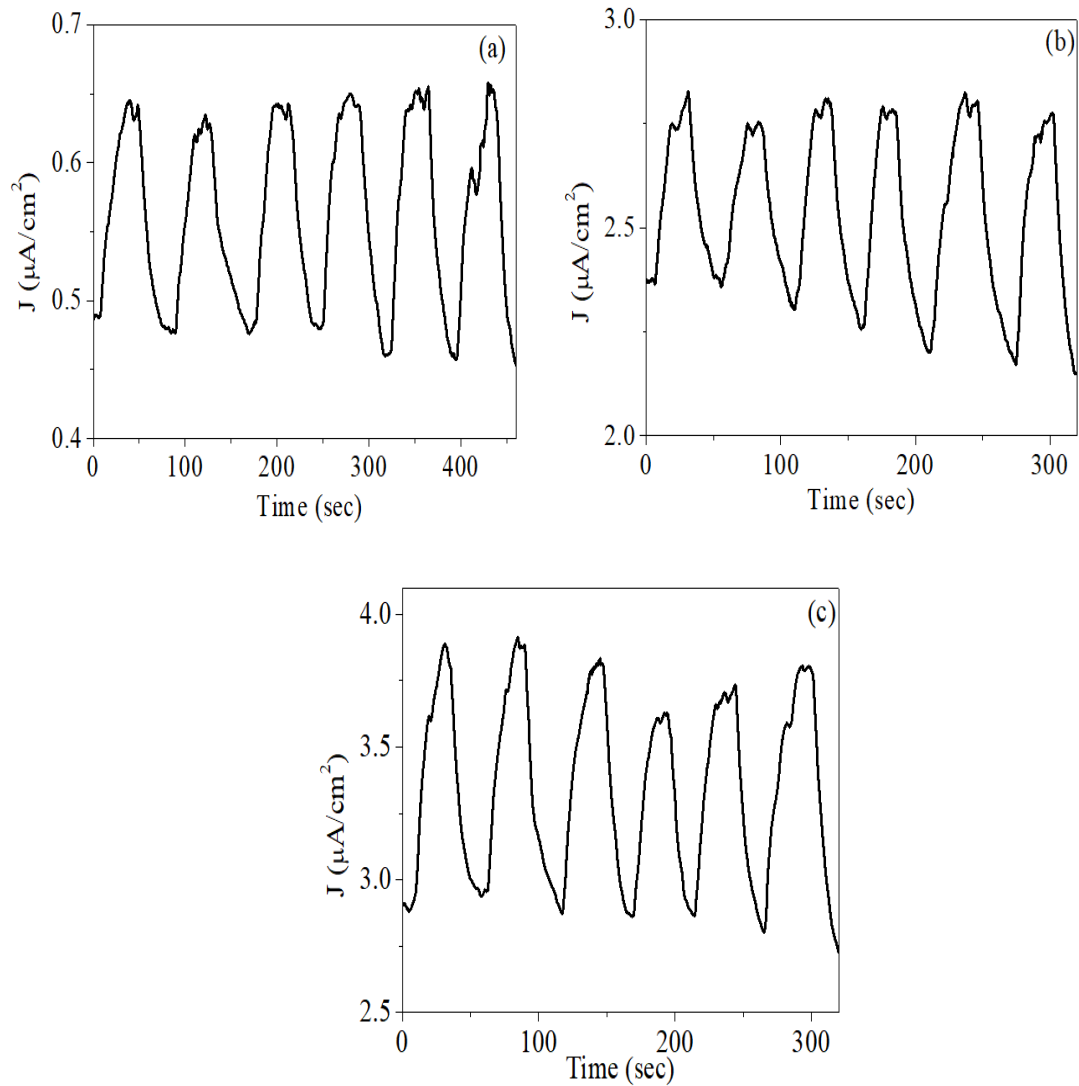


Fig. 8.2 UV response of (a) PVDF, (b) PVDF/ZnO films in relaxed and (c) PVDF/ZnO composite film in bend situation

For pristine PVDF film, dark current density of $\sim 0.47 \mu\text{A}/\text{cm}^2$ is observed at an external bias voltage of 10 V. But when UV light is incident upon them current gradually starts to rise and saturates at $\sim 0.64 \mu\text{A}/\text{cm}^2$ (fig. 8.2(a)). In similar condition, dark current of PVDF/ZnO composite is $\sim 2.22 \mu\text{A}/\text{cm}^2$ (fig. 8.2(b)). This rise in dark current is due to electrically conductive nature of ZnO inside PVDF/ZnO composite [202]. In presence of UV light, photocurrent rises to $\sim 2.78 \mu\text{A}/\text{cm}^2$. Therefore introduction of ZnO into PVDF considerably enhances both dark as well as UV induced photocurrent. Moreover, appropriate band gap of ZnO helps in further absorption in UV light. Average rise and fall times in this membrane are 21 sec and 27 sec respectively. Such slow response time in PVDF is attributed to high dielectric nature of such material [203]. On the other hand, ZnO is an inorganic, crystalline material capable of showing sharp response and recovery time [204]. When ZnO nanoparticles are loaded into PVDF polymer, rise and fall time slightly reduces to 18 sec and 21 sec respectively. This is due to interaction between ZnO surface charges and dipoles of PVDF which improves crystallinity of the composite [205]. Additionally, their flexibility allows them to operate even in Mechanically stressed situation. In mechanically stressed situation in form of bending dark and UV photocurrent further rises to ~ 2.87 and $3.73 \mu\text{A}/\text{cm}^2$ respectively (fig. 8.2(c)). This improved photoresponse is due to piezo-response of the composite. Thus PVDF/ZnO arises out to be better UV detecting composite along with flexibility.

Table – 8.1 UV photocurrent and response time of PVDF film, PVDF/ZnO composite film in bend and relaxed condition

| | J_{dark} ($\mu\text{A}/\text{cm}^2$) | J_{sat} ($\mu\text{A}/\text{cm}^2$) | Photocurrent ($\mu\text{A}/\text{cm}^2$) | Rise time (sec) | Recovery time (sec) | Responsivity ($\text{A}/\text{cm}^2/\text{W}$) |
|-----------------------|--|---|---|--------------------|------------------------|---|
| PVDF | 0.47 | 0.64 | 0.17 | 21 | 27 | 0.02 |
| PVDF/ZnO (Relaxed) | 2.22 | 2.78 | 0.56 | 18 | 21 | 0.06 |
| PVDF/ZnO (Bend) | 2.87 | 3.73 | 0.86 | 21 | 23 | 0.10 |

8.3. AC impedance spectroscopic analysis

AC impedance spectroscopic measurement has been performed for PVDF/ZnO composite in the frequency range of 5 Hz – 5 MHz by an external ac signal with 1 V of amplitude. Figure 8.3 represents variation of complex impedance with frequency in different external conditions. The composite exhibits a very high impedance of $\sim 78 \text{ M}\Omega$ at a frequency of 50 Hz which decreases rapidly with increase in frequency due to inability of dipoles to follow high frequency alteration. But when mechanical stress is applied in form of external bending, impedance falls greatly to $\sim 46 \text{ M}\Omega$ in similar circumstances. This huge fall in impedance is attributed to formation of additional charges on the grain surfaces due to distortion [206]. Impedance falls further around $\sim 40 \text{ M}\Omega$ in UV light exposure due to transfer of donor electrons to conduction levels of ZnO after absorption of UV light [207].

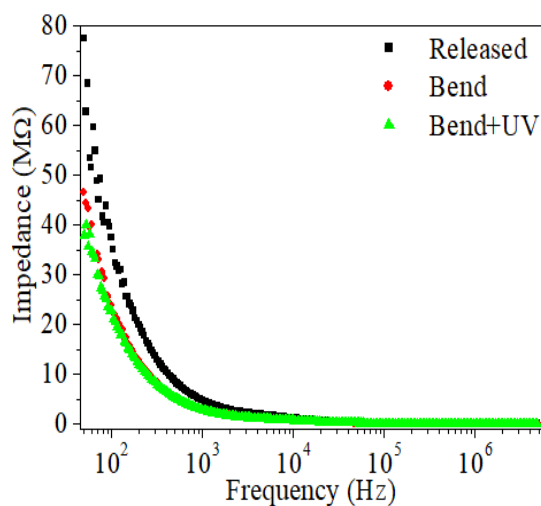


Fig. 8.3 Variation of impedance with frequency for PVDF/ZnO film in relaxed, bend and bend + UV illuminated condition

The parallel capacitance (C_p) becomes a crucial parameter describing electrical responses of those polymer composites since they possess very high impedance and low capacitance. Variation of C_p with frequency for the membrane in different external condition is shown in fig. 8.4. For

PVDF/ZnO composite, C_p is around 45 pF at 50 Hz frequency which falls rapidly with increasing frequency. This C_p arises due to obstruction offered by those barriers generated at boundaries [208]. Potential barrier at those boundaries appears due to difference in conductivity between grains and boundaries. Additionally, presence of ZnO creates more interfaces causing interfacial polarization to develop which acts as barrier and prevents movement of charges. Beyond a particular frequency, C_p seems to rise again slightly. This particular frequency is known as characteristics frequency when effects of interfaces become negligible and that of grains start to contribute. At such high frequency, orientational polarization becomes effective and storing capacity of grains become effective. Now those dipoles constituting grains of PVDF molecule start to respond to this frequency. When the composite is placed under some mechanical stress, C_p rises to ~ 65 pF. This rise in C_p is due to increment in polarization appears due to displacement of charges from their initial position. In this situation, when it is placed under UV irradiation C_p rise to ~ 75 pF due to generation of more charge carriers which face the obstruction at those boundaries due to formation of potential barrier there.

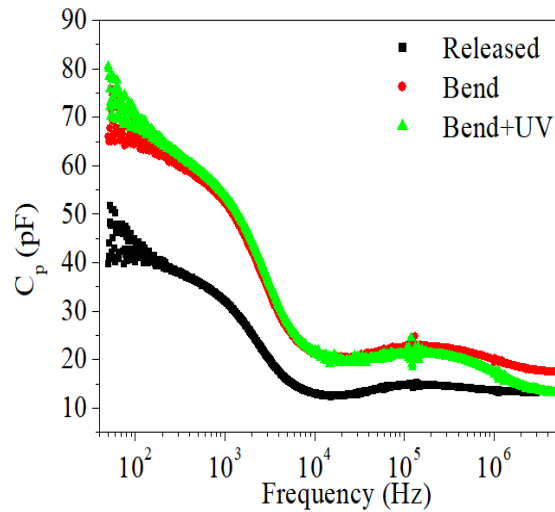


Fig. 8.4 Frequency vs C_p for PVDF/ZnO film in released, bend and bend + UV condition

Variation of real part of complex impedance (Z') and imaginary part of it (Z'') with frequency in different external situation are shown in fig. 8.5(a-b). Real part of complex impedance which is associated with ohmic resistance arises out to be ~ 20 M Ω at a frequency of 50 Hz. It shows a rapid fall with rise in frequency. This fall in Z' at high frequency is

attributed to increase in ac conductivity due to better hopping of electrons between separate grains [209]. Due to application of mechanical bending in form of bending Z' falls because of generation of additional dipoles participating in conduction mechanism. However in presence of UV light change in Z' is not so prominent. On the other hand Z'' which is associated with capacitive reactance of the composite shows a quick fall with frequency. Application of bending on the composite further lowers Z'' as bending introducing additional dipoles increasing the capacitance. In this situation when UV light is incident upon them Z'' reduces further hints towards additional carrier generation.

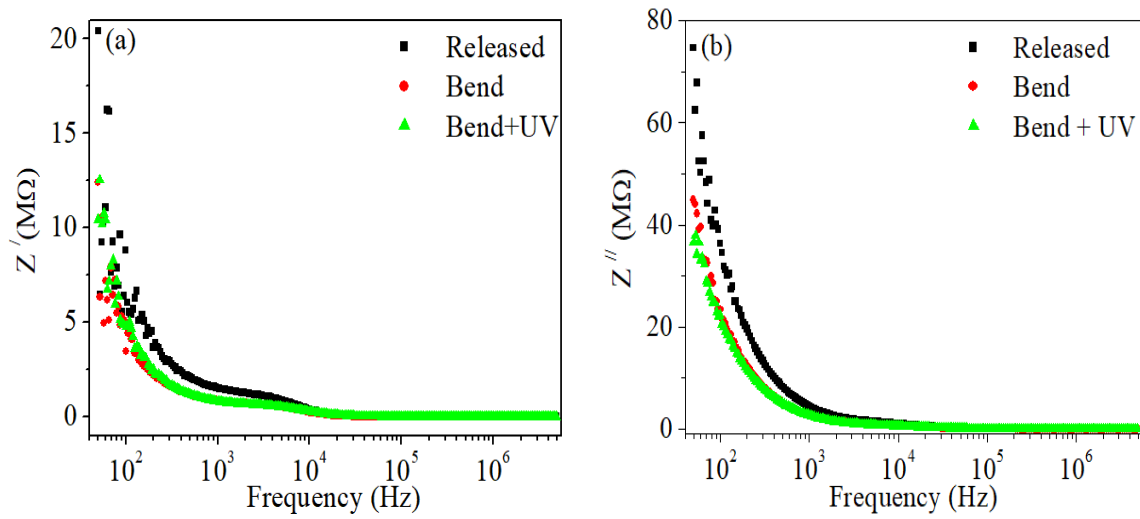


Fig. 8.5 (a) Frequency vs. Z' and (b) frequency vs. Z'' for PVDF/ZnO film in relaxed, bend and bend + UV irradiated condition

From the measured impedance spectroscopic data imaginary part of complex impedance (Z'') is plotted against real part of it (Z') in different external conditions and are shown in fig. 8.6(a-b). Here also two different segments are observed reveals two separate relaxation times exist in series [210]. Effect of bending on Nyquist plot is clearly visible from fig. 8.6(a). In low frequency region where effect of boundary is dominant, Z'' rises slightly due to enhancement of barrier potential at interfaces. Effect of boundary lasts a little longer because dipoles constituting grains starts resonating at slight higher frequency. From fig. 8.6(b) it is clear that when UV light is incident on them, Z'' is reduced only for that segment where effect

of boundary is dominant ensuring absorption of UV light by ZnO nanoparticles located at those boundaries.

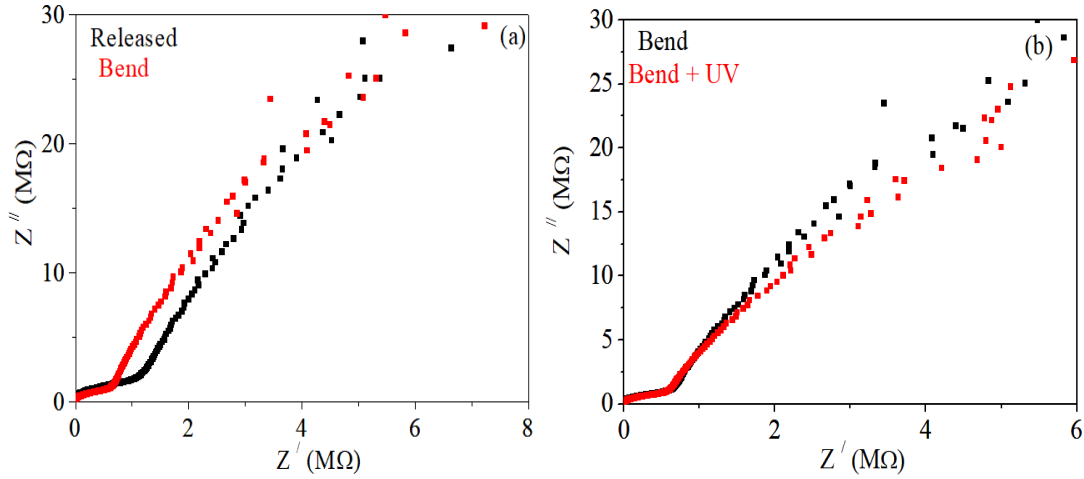


Fig. 8.6 Z'' vs. Z' for PVDF/ZnO film in (a) released and bend situation, (b) bend and bend + UV irradiated condition

These obtained Nyquist plots are fitted by previously mentioned electrical model circuit consisting of a series resistance with two parallel R-C circuits. Parameters of this model circuit are estimated by EIS spectrum analyzing software [187]. Experimentally obtained data and their corresponding fitted curves are shown in fig. 8.7. Extracted parameters from this fitting are presented in Table – 8.2. Using these parameters, two different relaxation times ($\tau_1 = R_1C_1$ and $\tau_2 = R_2C_2$) corresponding to grains at high frequency and interfaces at low frequency are estimated [190]. One those response times (τ_2) assigned to grains shows almost no change in external disturbances like mechanical bending or UV light irradiation. The other time constant (τ_1), which is assumed to be the effect of boundaries or interfaces, show significant change under external disturbances. Time constant τ_1 shows rise due to increment in interfacial polarization by bending. Also presence of UV light lowers the time constant because of generation of additional charge carriers in ZnO nanoparticles located at the boundaries which results in reduction in relaxation time.

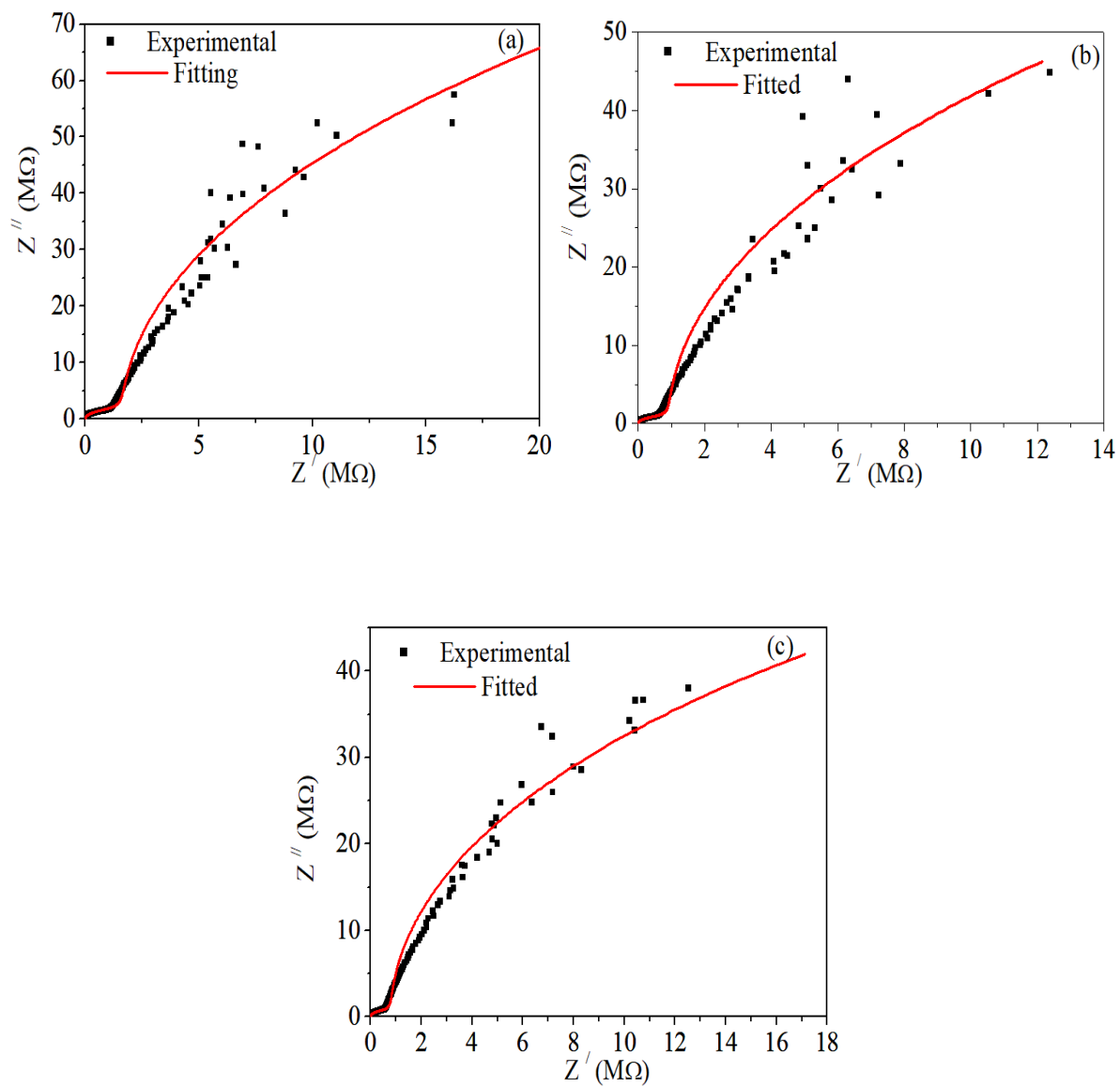


Fig. 8.7 Experimental and fitted curve for Nyquist plot of PVDF/ZnO film in (a) released (b) bend and (c) bend + UV condition

Table – 8.2 Fitting parameters for Nyquist plot of PVDF/ZnO in released, bend and bend + UV condition

| | $R_s(\Omega)$ | $R_1(\Omega)$ | $R_2(\Omega)$ | $C_1(F)$ | $C_2(F)$ | $\tau_1 = R_1C_1$ (sec) | $\tau_2 = R_2C_2$ (sec) |
|----------|---------------|--------------------|--------------------|------------------------|------------------------|----------------------------|----------------------------|
| Released | 450 | 2.53×10^8 | 1.62×10^6 | 4.13×10^{-11} | 2.06×10^{-11} | 10.4×10^{-3} | 3.3×10^{-5} |
| Bend | 531 | 2.01×10^8 | 9.25×10^5 | 6.49×10^{-11} | 3.08×10^{-11} | 13.0×10^{-3} | 2.8×10^{-5} |
| Bend +UV | 1087 | 1.23×10^8 | 7.96×10^5 | 6.58×10^{-11} | 2.78×10^{-11} | 8.0×10^{-3} | 2.2×10^{-5} |